

Cavity-linewidth narrowing by means of electromagnetically induced transparency

Hai Wang,* D. J. Goorskey, W. H. Burkett, and Min Xiao

Department of Physics, University of Arkansas, Fayetteville, Arkansas 72701

Received July 6, 2000

Cavity-linewidth narrowing in a ring cavity that is due to the high dispersion and reduced absorption produced by electromagnetically induced transparency (EIT) in rubidium-atom vapor has been experimentally observed. The cavity linewidth with rubidium atoms under EIT conditions can be significantly narrowed. Cavity-linewidth narrowing was measured as a function of coupling beam power. © 2000 Optical Society of America

OCIS codes: 270.1670, 260.2030, 140.4480, 020.1670, 260.5740, 300.3700.

Generally, laser light passing through an atomic medium will be strongly absorbed if the laser frequency is near a transition frequency of the atoms. Recently, however, it was demonstrated¹⁻⁴ that, because of atomic coherence in multilevel atomic systems, the transparency of the medium to a probe beam near an atomic transition frequency can be controlled by a second coupling beam interacting with another atomic transition. This effect, known as electromagnetically induced transparency (EIT), has attracted great attention because of the properties of large dispersion and almost-vanishing absorption in such systems.¹⁻⁵ More recently, EIT systems were used to achieve ultraslow group velocity of light.⁵⁻⁸ Whereas some theoretical calculations have been made that predicted such effects as optical bistability,⁹ frequency pulling, and linewidth narrowing¹⁰ for an EIT system inside an optical cavity, we are aware of no reported experiments to demonstrate these interesting effects. In this Letter we report the experimental observation of cavity-linewidth narrowing of an optical ring cavity with three-level Λ -type rubidium atoms inside. Typically, an absorbing medium inside an optical cavity will increase the cavity linewidth. However, because of the large dispersion change and reduced absorption in the EIT system, the cavity linewidth can be significantly narrowed.

We consider a three-level Λ -type atomic system, as shown in Fig. 1, within a heated vapor cell of length l in an optical ring cavity of length L . The susceptibility χ of the medium to a probe beam of frequency ω_p can be separated into real (χ') and imaginary (χ'') parts. The real part gives the dispersion $\partial\chi'/\partial\omega_p$, and the imaginary part gives the absorption coefficient $\alpha = (n_0\omega_p/c)\chi''$, where n_0 is the background index of refraction. Owing to the dispersion of the intracavity medium, the resonant frequency ω_r of the cavity with the Rb vapor cell is pulled according to the relation¹⁰

$$\omega_r = \frac{1}{1 + \eta} \omega_e + \frac{\eta}{1 + \eta} \omega_{21}, \quad (1)$$

where $\omega_e = mc/L$ (for integer m) is the resonant frequency of the empty cavity and ω_{21} corresponds to the probe transition frequency of the Rb atoms. $\eta = \omega_r(l/2L)(\partial\chi'/\partial\omega_p)$ describes dispersion changes as a

function of probe frequency. By considering both the absorption and the dispersion of the medium simultaneously, one can show that the ratio of the linewidth $\Delta\omega$ of the cavity with the medium to that of the empty cavity is¹⁰

$$\frac{\Delta\omega}{C} = \frac{1 - R\kappa}{\sqrt{\kappa}(1 - R)} \frac{1}{1 + \eta}, \quad (2)$$

where C is the linewidth of the empty cavity and R is the reflectivity of both the input and the output mirrors; $\kappa = \exp(-\alpha l)$ describes the absorption of the medium per pass. In a two-level system, when the cavity plus medium resonant frequency ω_r is close to the natural resonant frequency ω_{21} of the Rb atoms, dispersion $\partial\chi'/\partial\omega_p$ becomes larger, which causes narrowing of the cavity linewidth; but, at the same time, absorption χ'' also becomes larger near resonance, which cancels the narrowing effect. If, however, an EIT occurs in three-level Rb atoms, the absorption is reduced and a larger dispersion is created,⁵ which results in a substantial narrowing of the cavity linewidth.

In the experiment, the Rb atoms, as shown in Fig. 1, interact with a weak (probe) laser field with Rabi frequency $\Omega_1 = -\mu_{21}E_1/\hbar$ and a strong (coupling) laser field of Rabi frequency $\Omega_2 = -\mu_{23}E_2/\hbar$, where E_1 and E_2 are the strengths of the respective fields and μ_{21} and μ_{23} are the relevant dipole moments. The complex susceptibility of the EIT system is given by⁴

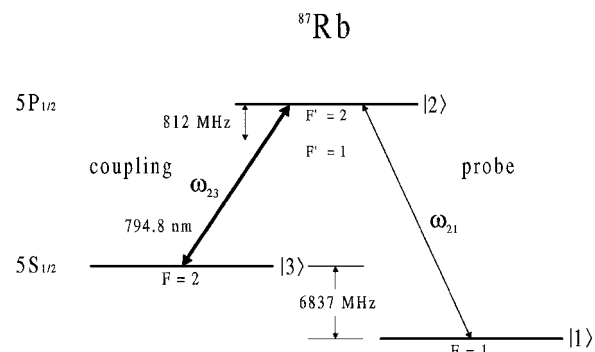


Fig. 1. Diagram of the three-level Λ -type system in the D_1 line of ^{87}Rb .

$$\chi = \frac{ic\mu_{21}^2 N_0 \sqrt{\pi}}{\epsilon_0 \hbar \omega_p u} e^{z^2} [1 - \text{erf}(z)], \quad (3)$$

with the argument that

$$z = \frac{c}{\omega_p u} \left[\gamma - i\Delta_1 + \frac{\Omega_2^2/4}{\Gamma_3 - i(\Delta_1 - \Delta_2)} \right], \quad (4)$$

where $\text{erf}(z)$ is the error function, $N_0 = N_0(T)$ is the temperature-dependent atomic density function, ω_p is the frequency of the probe laser, and $u/\sqrt{2}$ is the root-mean-square atomic velocity: $u = \sqrt{2k_B T/m}$. Here, $\gamma = (\Gamma_1 + \Gamma_2 + \Gamma_3)/2$, where Γ_1 and Γ_2 are the spontaneous decay rates of excited state $|2\rangle$ to ground states $|1\rangle$ and $|3\rangle$, respectively, and Γ_3 is the nonradiative decay rate between the two ground states. Also, $\Delta_1 = \omega_p - \omega_{21}$ is the detuning of the probe field from atomic transition frequency ω_{21} between levels $|1\rangle$ and $|2\rangle$. $\Delta_2 = \omega_c - \omega_{23}$ is the detuning of the coupling field from the atomic transition frequency ω_{23} between levels $|2\rangle$ and $|3\rangle$, which is kept on resonance throughout the experiment, so $\Delta_2 = 0$. One may take the laser linewidths into account³ by including them in the decay rates such that $\gamma \rightarrow \gamma + \delta\omega_p$ and $\Gamma_3 \rightarrow \Gamma_3 + \delta\omega_p + \delta\omega_c$, where $\delta\omega_p$ and $\delta\omega_c$ are the half-linewidths of the probe and coupling lasers, respectively.

A diagram of the experimental setup is shown in Fig. 2. Both the coupling and the probe lasers are single-mode tunable Hitachi HL7851G diode lasers that are current and temperature stabilized. The probe laser frequency is further stabilized with a weak grating feedback in the Littrow configuration,¹¹ which yields a probe laser half-linewidth of $\delta\omega_p \approx 1.0$ MHz. The coupling laser (free-running) has a half-linewidth of $\delta\omega_c \approx 2.1$ MHz. Polarizing beam splitters PB2 and PB4 separate $\sim 10\%$ of the coupling and probe beams into an auxiliary Rb cell (combined through PB3) followed by a Fabry-Perot cavity and a detector for measuring the absorption and monitoring laser frequency hopping. The remaining beams are brought together by beam splitter PB1 and focused at the center of a 5-cm-long Brewster-cut Rb cell with μ metal wrapped in heat tape in one arm of the optical ring cavity. The transmissivities of flat mirror M1 and concave mirror M2 are approximately 2% and 3%, respectively. The third cavity mirror (PZT) with a reflectivity of 99.5% is also concave and is controlled by a piezoelectric driver. Both concave mirrors have a 10-cm radius of curvature. The finesse of the empty cavity (without the Rb cell and a polarizing beam splitter) is 100. The free spectral range of the empty cavity (36.5 cm in length) is 822 MHz, so empty-cavity linewidth C is $2\pi \times 8.22$ MHz. The coupling and probe beams are orthogonally polarized when they enter the ring cavity through PB1 and propagate collinearly. The probe beam and the coupling beam are focused into the cavity by lenses with focal lengths of 15 and 40 cm, respectively, and their respective beam diameters at the center of the Rb vapor cell are estimated to be 140 and 280 μm . The coupling beam is rejected by PB5 before reaching detector D2. After

the Rb cell and PB1 are inserted, because of surface reflection losses the finesse of the cavity (with the Rb atoms off resonance) is reduced to 51.

Experimental measurements were conducted as follows: First, mirror M2 was removed and the probe beam frequency was scanned near ω_{21} in a range of approximately $2\pi \times 770$ MHz with a scanning time of 8.5 ms with a zigzag current driver operating with a peak-to-peak voltage of 5 mV. The frequency of the coupling beam was tuned to atomic transition frequency ω_{23} until the characteristic EIT absorption dip⁴ was observed and centered. Mirror M2 was then put back to form the ring cavity. We adjusted the cavity length to match resonant frequency ω_r of the cavity plus medium to resonant frequency ω_{21} of the Rb atoms by changing the driving voltage of the PZT-mounted mirror. When this condition ($\omega_e = \omega_{21} = \omega_r$) is met, the transmission peak is highest and narrow. Figure 3 shows a comparison of the cavity linewidth for a probe frequency well off the absorption line without the coupling beam and of the cavity linewidth when

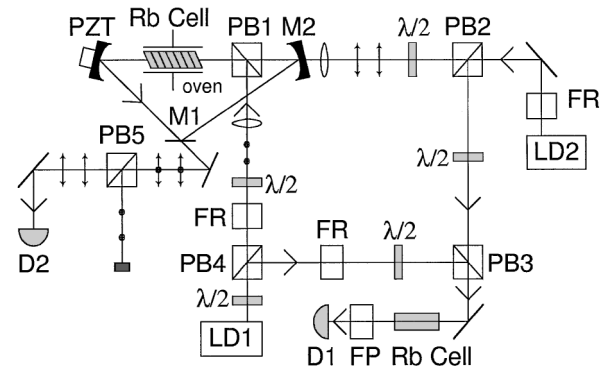


Fig. 2. Experimental setup: LD1, LD2, coupling and probe lasers, respectively; PB1–PB5, polarizing cubic beam splitters; $\lambda/2$'s, half-wave plates; FR's, Faraday rotation isolators; FP, Fabry-Perot cavity; D1, D2, detectors; other abbreviations defined in text.

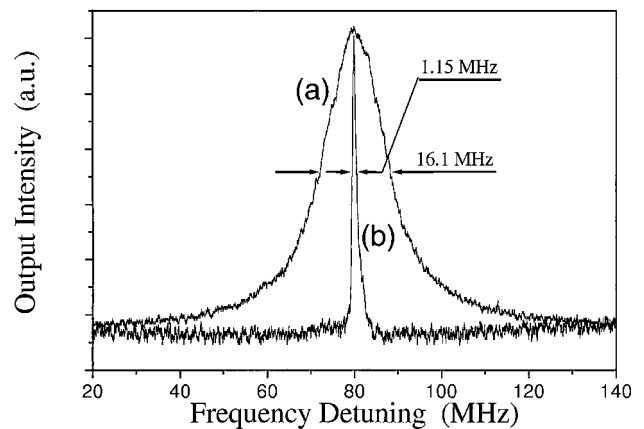


Fig. 3. Intensity of cavity output versus probe frequency, showing cavity-length narrowing. Note that the intensity scales are different for curves (a) and (b). $T = 87^\circ\text{C}$. (a) No coupling beam ($\Omega_2 = 0$); probe frequency well outside the absorption line. (b) With the coupling field on and the probe frequency scanned through the probe transition. Coupling power, 0.81 mW; $\Delta_2 = 0$.

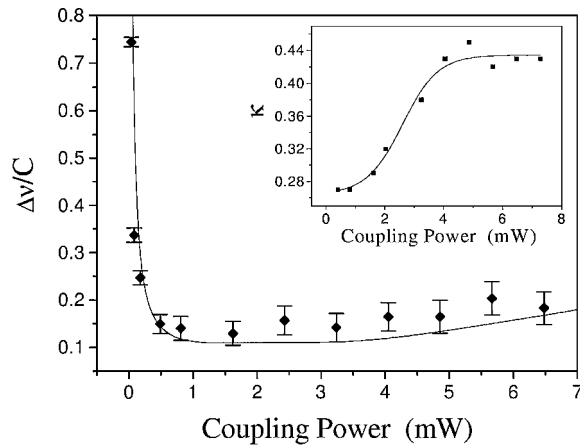


Fig. 4. Ratio of EIT-narrowed cavity linewidth $\Delta\nu$ to empty-cavity linewidth C as a function of coupling power. Points, experimentally measured with $T = 87^\circ\text{C}$ and an intracavity Rabi frequency of $\Omega_p = 2\pi \times 4.9$ MHz. Solid curve, calculated from Eq. (2) with $\Gamma_3 = 2\pi \times 3.2$ MHz, $\gamma = 2\pi \times 4.0$ MHz, and a coupling beam diameter of $280\ \mu\text{m}$ at its waist. Inset, κ versus coupling power for $T = 87^\circ\text{C}$.

the cavity field is tuned to the probe transition with the coupling beam. The coupling laser power entering the Rb vapor cell was ~ 0.81 mW (corresponding to a Rabi frequency of $\Omega_c = 2\pi \times 49.8$ MHz), and the probe laser Rabi frequency at the center of the cell was approximately $\Omega_p = 2\pi \times 4.9$ MHz. The cavity linewidth for the cavity containing the Rb vapor cell and the beam splitter but with no coupling beam and with the probe frequency tuned off resonance was $C' = 2\pi \times 16.1$ MHz. With the coupling beam on and the probe beam tuned to the probe transition, the linewidth was $2\pi \times 1.15$ MHz, which is a factor of 14 narrower than cavity linewidth C' and a factor of 7 narrower than empty-cavity linewidth C .

We also measured the dependence of the cavity linewidth on the intensity of the coupling beam, as shown in Fig. 4. The Rb vapor cell was kept at a constant temperature of approximately 87°C . We calculated the theoretical curve from Eq. (2), assuming a temperature-dependent density function $N_0(T)$ (given elsewhere¹²) and a coupling beam diameter of $280\ \mu\text{m}$ at its waist inside the cell. Transmission κ was measured experimentally (Fig. 4, inset) and included in the calculated curve because Eqs. (2) and (3) do not take into account high-density absorptive behavior. The theoretical curve is in good agreement with experimental data. For low coupling powers the cavity linewidth is broad because the EIT and sharp dispersion will not be fully developed. As the coupling power increases, the cavity linewidth narrows rapidly until it reaches a minimum at approximately 1–3 mW. When the coupling power is increased further, the linewidth slowly broadens again, which is a result of power broadening of the resonance.

The current experimentally achieved cavity-linewidth narrowing is limited by several factors. The dominant one at this stage is the linewidths of

the coupling and probe lasers. Other limiting factors include intracavity losses that are due to the surfaces of the vapor cell and the polarizing beam splitter, laser frequency stability, and mechanical vibration of the optical cavity. With further technical improvements, we can expect to achieve cavity-linewidth narrowing factors of 10^3 – 10^4 in accordance with the slowing of the group velocity of light to a mere few meters per second.^{6–8}

In conclusion, we have experimentally demonstrated cavity-linewidth narrowing by means of electromagnetically induced transparency with atomic-Rb vapor in an optical ring cavity. Experimental results show that the cavity linewidth narrows rapidly with coupling power up to a point and then broadens again slowly because of power broadening. The cavity linewidth is narrower by a factor of 7 than empty-cavity linewidth C and by a factor of 14 than cavity linewidth C' with intracavity losses. This technique can have potential applications in high-resolution spectroscopy and laser frequency stabilization. This effect provides an interesting way to control the cavity linewidth by use of another laser beam. It will be interesting to apply this cavity-linewidth narrowing effect in an optical cavity with an active medium (a laser system). With substantial linewidth narrowing, one might suppress the phase fluctuations of a laser beyond the shot-noise limit.

We acknowledge funding support from the U.S. Office of Naval Research and the National Science Foundation. M. Xiao's e-mail address is mxiao@comp.uark.edu.

*Permanent address, Institute of Optoelectronics, Shanxi University, Taiyuan 030006, China.

References

1. K. J. Boller, A. Imamoglu, and S. E. Harris, *Phys. Rev. Lett.* **66**, 2593 (1991).
2. S. E. Harris, *Phys. Today* **50**(7), 36 (1997), and references therein.
3. J. Gea-Banacloche, Y.-C. Li, S.-Z. Jin, and M. Xiao, *Phys. Rev. A* **51**, 576 (1995).
4. Y.-Q. Li and M. Xiao, *Phys. Rev. A* **51**, R2703 (1995).
5. M. Xiao, Y.-Q. Li, S.-Z. Jin, and J. Gea-Banacloche, *Phys. Rev. Lett.* **74**, 666 (1995).
6. L. V. Hau, S. E. Harris, Z. Dutton, and C. H. Behroozi, *Nature* **397**, 594 (1999).
7. M. M. Kash, V. L. Sautenkov, A. S. Zibrov, L. Hollberg, G. R. Welch, M. D. Lukin, Y. Rostovtsev, E. S. Fry, and M. O. Scully, *Phys. Rev. Lett.* **82**, 5229 (1999).
8. D. Budker, D. F. Kimball, S. M. Rochester, and V. V. Vashchuk, *Phys. Rev. Lett.* **83**, 1767 (1999).
9. W. Harshawardhan and G. S. Agarwal, *Phys. Rev. A* **53**, 1812 (1996).
10. M. D. Lukin, M. Fleishhauer, M. O. Scully, and V. L. Velichansky, *Opt. Lett.* **23**, 295 (1998).
11. S.-Z. Jin, Y.-Q. Li, and M. Xiao, *Appl. Opt.* **35**, 1436 (1996); K. B. MacAdam, A. Steinbach, and C. Weiman, *Am. J. Phys.* **60**, 1098 (1992).
12. A. G. Truscott, M. E. J. Friese, N. R. Heckenberg, and H. Rubinsztein-Dunlop, *Phys. Rev. Lett.* **82**, 1438 (1999).